JACS
JOURNAL OF THE AMERICAN CHEMICAL SOCIETY

Communication

pubs.acs.org/JACS

Excess Electron Interactions with Solvated DNA Nucleotides: Strand Breaks Possible at Room Temperature

Maeve Smyth and Jorge Kohanoff*

Atomistic Simulation Centre, Queen's University Belfast, Belfast BT7 1NN, U.K.

Supporting Information

ABSTRACT: When biological matter is subjected to ionizing radiation, a wealth of secondary low-energy (<20 eV) electrons are produced. These electrons propagate inelastically, losing energy to the medium until they reach energies low enough to localize in regions of high electron affinity. We have recently shown that in fully solvated DNA fragments, nucleobases are particularly attractive for such excess electrons. The next question is what is their longer-term effect on DNA. It has been advocated that they can lead to strand breaks by cleavage of the phosphodiester $C_{3'}$–$O_{3'}$ bond. Here we present a first-principles study of free energy barriers for the cleavage of this bond in fully solvated nucleotides. We have found that except for dAMP, the barriers are on the order of 6 kcal/mol, suggesting that bond cleavage is a regular feature at 300 K. Such low barriers are possible only as a result of solvent and thermal fluctuations. These findings support the notion that low-energy electrons can indeed lead to strand breaks in DNA.

Understanding the effects of ionizing radiation in biologically relevant systems is crucial in fully assessing the dangers posed by radiation and understanding how to improve its efficiency in combating cancer. Despite the extensive progress made in examining the effects of secondary low-energy electrons (LEEs),[1,2] there is still much to be learned. An abundance of important experimental and theoretical studies on *dry* DNA have been done,[3−6], but the extension to a more realistic environment that includes water and proteins and is subject to solvent and thermal fluctuations is not obvious. This communication highlights the importance of trying to reach a more realistic model of DNA damage. This was achieved by means of first-principles room-temperature simulations of the interactions of LEEs with DNA nucleotides solvated by explicit water molecules, which were treated at the same level of theory as the nucleotides. Our results show that a prehydrated electron can cause strand breaks in this environment.

In pure water, excess electrons are localized in cavities exhibiting a deep potential well; the binding energy is −3.2 eV.[7] However, the state of excess electrons before hydration is under debate. Wang et al.[8] recently used femtosecond time-resolved laser spectroscopy, which can detect these so-called *prehydrated* electrons (e^-_{pre}), to show that there are two intrinsic e^-_{pre} states with lifetimes of 180 and 550 fs. This work was extended to a study of the solvation of nucleotides in water,[9] where an excess electron was generated by double excitation of a water molecule with UV photons. These authors detected excited anionic states of the nucleotide, implying that ionization of the water molecule had occurred. The subsequent reactions may be expressed as e^-_{pre} + dXMP → $(dXMP^-)^*$ → $dXMP^-$ or dissociation products, where dXMP is the nucleotide and X is one of the four nucleobases T, C, G, and A. These states were formed within the lifetime of e^-_{pre}. It was documented that all of the bases attracted an excess electron. However, A and C formed *stable* anionic species, whereas T and especially G dissociated in proportions of 35 and 60%, respectively. This fragmentation occurred within 2 ps, suggesting that the cleavage proceeds via the transient negative ion state rather than the stable one.

Many theoretical studies have been carried out to explain the mechanism of DNA strand breakage by excess electrons.[10−20] The process can be divided into two steps. In the first, the electron attaches to the nucleotide and then is transferred to specific bonds along the backbone, facilitating their cleavage. Electron attachment to nucleotides in both the gas phase and aqueous solution was thoroughly studied during the past decade.[10−16] The comprehensive comparative study of Gu et al.[16] concluded that in the gas phase, the adiabatic electron affinity of nucleotides reaches values of 0.2−0.5 eV, which are significantly enhanced relative to those of the nucleobases. The excess electron appears to be delocalized between the base and the phosphate. When solvation effects were introduced at an implicit level using the polarizable continuum model (PCM), the electron affinities dramatically increased to values of ∼2 eV with the excess electron localized in the base, except for the guanosine nucleotide (dGMP), which exhibited an affinity of 1 eV with the electron localized at the phosphate end. The PCM solvation model does not include specific interactions such as H-bonding to water molecules and thus can miss some important features. To address this, Schyman and Laaksonen compared electron attachment to dGMP using PCM solvation or inclusion of a first solvation shell of explicit water molecules.[20] The excess electron was observed to be localized in a dipole-bound state around the guanine, protruding into the solvent region beyond the first solvation shell.

The second step, bond cleavage induced by electron attachment, was also studied at length by various authors. The three main pathways for bond cleavage in nucleotides involve the phosphodiester linkages between the sugar and phosphate at the 3′ and 5′ positions and the N-glycosidic $C_{1'}$–N_1 bond between the sugar and the base (Figure 1).

Received: April 19, 2012
Published: May 18, 2012

   dx.doi.org/10.1021/ja303776r | J. Am. Chem. Soc. 2012, 134, 9122−9125

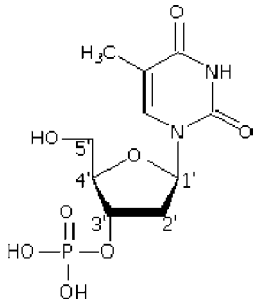

Figure 1. Molecular structure of thymidine monophosphate.

Calculations on pyrimidine nucleotides[13,17] showed that the $C_{3'}-O_{3'}$ bond has the lowest gas-phase activation energy (6−7 kcal/mol), while the barriers for cleavage at the 5′ position and at the N-glycosidic bond are significantly higher (13−14 and 20−26 kcal/mol, respectively). Similar activation barriers were recently reported for the adenosine nucleotide,[18] but as before, guanosine appears to have different properties.[21] Upon PCM solvation, the $C_{3'}-O_{3'}$ barriers increased to 13−14 kcal/mol for T, C, and A[17,18] but remained as low as 3−4 kcal/mol for G.[21] Explicit microsolvation was considered for dGMP,[20] and no significant differences in the activation barrier relative to PCM solvation were observed. The barrier was reported to decrease from ∼10 kcal/mol in the gas phase to ∼5 kcal/mol (PCM) or ∼7 kcal/mol (explicit), in contrast to the results of Gu et al.[21]

In summary, the activation energy for the $C_{3'}-O_{3'}$ bond cleavage was reported to increase significantly upon solvation, thus leading to the conclusion that strand breaks are less likely to occur in the condensed phase, with the exception of dGMP. It is important to remark that all of these studies were conducted at T = 0 K by optimizing the structure of the nucleotides while constraining the length of the $C_{3'}-O_{3'}$ bond at different values. Therefore, the barriers do not take into account the entropic contribution from the electrostatic and thermal fluctuations of the aqueous environment. Another relevant aspect of these calculations is that the model nucleotides considered are closed-shell species neutralized with a proton or a methyl group, so the excess electron goes into a singly occupied molecular orbital (SOMO).

The fluctuating aqueous environment was considered explicitly in a hybrid quantum mechanical/molecular mechanical (QM/MM) molecular dynamics (MD) simulation of the cytidine nucleotide in which the water molecules were treated classically.[22] In this simulation, the authors studied a negatively charged solvated nucleotide rather than the neutral form. The main conclusion was that even if the excess electron did somehow lower the barriers, these remained at ∼30 kcal/mol, so bond cleavage at room temperature was unfavorable. An aspect of these simulations was that electrons were not allowed into the MM region and thus were forced to localize in the LUMO of the nucleotide.

To make progress in the study of strand breaks due to excess electrons, it is necessary to consider DNA fragments in a realistic, thermally fluctuating environment. Moreover, the surrounding environment has to be modeled at the same level as the DNA. This serves two purposes: On one hand, it allows the excess electron to be partially localized in the water orbitals, if necessary. In fact, in a previous study, we observed that the surrounding water orbitals help stabilize the excess charge in nucleobases and nucleosides by participating in the SOMO.[23] On the other hand, it allows for protonation of the nucleotide because, at variance with most classical models, QM water molecules can dissociate. This is extremely relevant because protonation is a competing mechanism for bond cleavage; it tends to stabilize the excess electron by neutralizing the system. With this in mind, we endeavored to simulate cleavage of the $C_{3'}-O_{3'}$ bond due to excess electrons for each of the explicitly solvated nucleotides at room temperature.

We constructed a model of each system by adding 100 water molecules around a central nucleotide.[24] After equilibrating the system with a classical MD simulation of the periodically repeated box using DL_POLY,[25] we chose representative reference frames as starting points for first-principles MD simulations using the ab initio Quickstep module of the CP2K package.[26] The electronic structure was computed within density functional theory using the Gaussian and augmented plane waves method. This automatically imposes periodic boundary conditions, thus allowing for condensed-phase calculations. In gas-phase calculations, periodic images were decoupled as in ref 27. Core electrons were replaced by GTH pseudopotentials[28], and a triple-ζ plus polarization basis set (TZVP-GTH) was employed. We used the PBE exchange−correlation functional,[29] which was checked against the corresponding hybrid functional PBE0 for gas-phase calculations (see the Supporting Information for details).

We considered two aspects of the problem: the presence of the explicit solvent and the thermal fluctuations of the molecule and the environment. At T = 0 K, we computed the ground-state energy by fixing the value of the reaction coordinate and minimizing the energy with respect to all remaining degrees of freedom. This was done in both the gas and condensed phases. For T > 0 K, the relevant thermodynamic potential is the free energy, which takes into account energy exchanges with the environment. Free energy barriers for the phosphodiester bond cleavage were obtained using constrained MD simulations (using the $C_{3'}-O_{3'}$ bond as the reaction coordinate) and thermodynamically integrating the constraint force.[30] An important technical aspect was to ensure that solvent fluctuations were properly sampled, as these degrees of freedom alter the bonding forces between the atoms.

Our MD simulations were conducted at 300 K to mimic the ambient conditions under which this system would naturally thrive. To this end, we simulated the periodic system at constant V and T for an equilibration period of 2 ps followed by 2.5 ps of production time. We checked the fluctuations in the energy and constraint forces to ensure that equilibration was achieved and that the statistical averages were stable. The electronic motion was described within the adiabatic approximation, with the electronic density following the nuclear dynamics instantaneously. Thus, excited states were not included in this work. Finally, in our model, one of the oxygens in the phosphate group was protonated to render the system neutral. Protonation of the nucleotide is not expected to affect the energetics.[12] Moreover, at the first-principles level, protonation and deprotonation occur spontaneously during the dynamics following solvent fluctuations.

We first examined the interaction of a vertically attached 0 eV electron with our condensed-phase system. In agreement with experiment,[9] we found that the electron effectively attaches to the nucleotides, giving rise to anionic species. This extends our previous study on nucleobases and nucleosides,[23] in which the electron was seen to localize around the nucleobase in times on the order of 15−25 fs. The localization time scale for nucleotides, which is dictated by the dynamics of the small

dx.doi.org/10.1021/ja303776r | J. Am. Chem. Soc. 2012, 134, 9122−9125

geometric rearrangements required to accommodate the excess electron, remained essentially the same. In Figure 2, we show

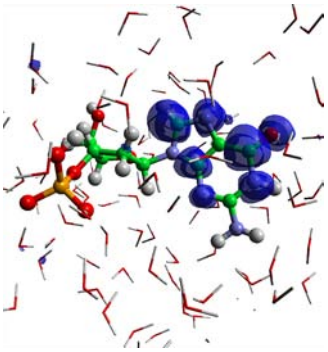

Figure 2. Spin density of guanosine monophosphate upon excess electron attachment. The electron is localized in the base, with no signature of a dipole-bound state as observed with a PCM solvent[21] and under microsolvation.[20]

the spin density (very similar to the SOMO) for the controversial dGMP, but now fully solvated with QM water molecules. The resulting density was clearly localized in the guanine, with no protruding lobes indicating a dipole-bound state. The spin densities for the other nucleotides were similar in character. We did not observe spontaneous bond cleavage during these unconstrained simulations, thus indicating that the process must be activated.

In agreement with previous studies,[10,11,13,14,17] we found the gas-phase activation energies of the bases to be 4−5 kcal/mol (Table 1). Similarly, we observed the addition of explicit

Table 1. Barrier Heights for Each of the Nucleotides[a]

		condensed phase	
nucleotide	gas phase (0 K)	0 K	300 K
dTMP	4.2	13.2	6.3
dCMP	4.7	14.5	5.9
dGMP	5.0	15.2	6.2
dAMP	4.8	12.0	10.4

[a]Values in kcal/mol. Condensed-phase values at 0 K are upper bounds obtained by local energy minimizations starting from representative frames. The uncertainty in the free energies at 300 K is ∼1 kcal/mol.

solvation effects at a static level to raise this energy to 12−15 kcal/mol, as with implicit PCM solvent. The barrier for T = 0 K condensed-phase dTMP reached a maximum value of 13.2 kcal/mol at a bond length of ∼1.75 Å. It was the inclusion of explicit solvent fluctuations at 300 K that lowered the barrier again to levels comparable to the gas-phase values. The computed free energy barrier was 6.3 kcal/mol at a slightly stretched bond length of 1.8 Å.

We calculated free energy profiles for all of the nucleotides (Figure 3) to enable comparison of all cases within the same theoretical framework. Upon addition of a 0 eV electron, all of the solvated nucleotides exhibited low free energy barriers of 5−10 kcal/mol. These barriers are sufficiently low to allow for the cleavage of the $C_{3'}$−$O_{3'}$ bond at room temperature. In all cases, static solvation appeared to stabilize the electron in the nucleobase, raising the energy barriers by ∼10 kcal/mol. Except for the adenosine nucleotide, these barriers returned to ones comparable to the gas-phase values once thermal fluctuations

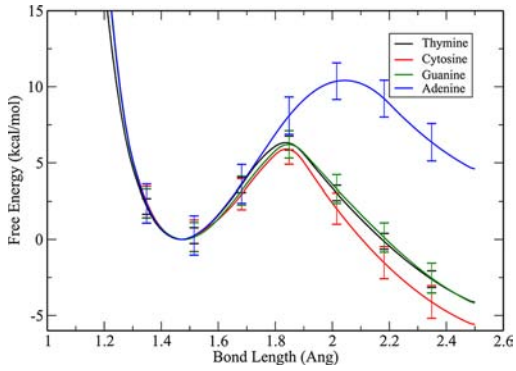

Figure 3. Free energy profiles as functions of the $C_{3'}$−$O_{3'}$ bond length for dTMP (black), dCMP (red), dGMP (green), and dAMP (blue).

were included. This would suggest that the latter allows for some additional freedom of movement of the excess electron, thus making the strand breaking process easier.

dAMP is the clear exception, with a free energy barrier of 10.4 kcal/mol at an elongated bond length of 2 Å. On closer examination, the adenine was in fact found to be protonated during the simulation at a constrained bond length of 1.7 Å. At 2 Å, the electron is attracted toward the $C_{3'}$ position, and the adenine deprotonates because it is no longer charged. This barrier is significantly higher than for the other bases, suggesting that the DNA strand is unlikely to break close to adenosine nucleotides. This result partially explains the experiments of Wang et al.,[9] which highlighted A and C as sites where strand breaks do not occur. It does not explain why the cytidine nucleotide is not prone to cleave upon electron addition. Although we did not see this in our simulations, it has been suggested that cytosine also readily becomes protonated once it captures an electron, thus inhibiting further reactions[31] (see the discussion at the end of ref 18). In fact, protonation and strand breaking are competing channels, and it is plausible that protonation is faster than bond cleavage. A study of this competition for the various nucleotides was beyond the scope of the present work but is certainly very important and will be subject of future studies. Deprotonation of the phosphate may also lead to an enhanced barrier, as observed in QM/MM calculations.[22] Further investigations will be carried out in this regard. Another aspect to consider is that in this experiment the electron is promoted from an orbital of a neighboring water molecule into an excited, fairly delocalized e^-_{pre} state having some spare energy (a few eV) that can go into vibrational motion, which promotes dissociation. Also, the potential energy surface is modified and the bond weakened by the population of antibonding orbitals. Our simulations did not include any of these possibilities as they were based on the Born−Oppenheimer approximation describing the electronic ground state.

Simons[19] showed that when the $C_{3'}$−$O_{3'}$ bond is elongated beyond 1.85 Å, there is a level crossing between the occupied π^* orbital in the nucleobase and an empty σ^* phosphodiester bond orbital; transfer of the electron weakens the bond, promoting its cleavage. To analyze whether this picture remains valid in the fluctuating environment, we examined the motion of the excess electron during the constrained dynamics. Figure 4 shows representative snapshots of the spin density for three bond lengths. The left panel is for 1.4 Å, which is near the equilibrium. The electron is located in the nucleobase. The middle panel is for a bond length of 1.8 Å, in the region of the

dx.doi.org/10.1021/ja303776r | J. Am. Chem. Soc. 2012, 134, 9122−9125

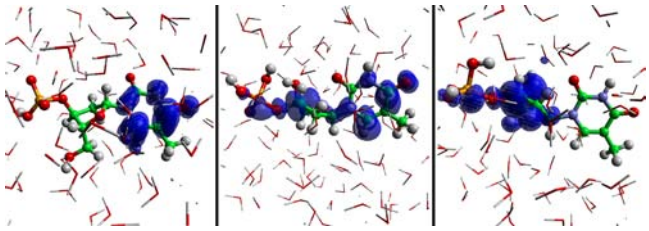

Figure 4. Spin density plots for deoxythymidine monophosphate: (left) at the equilibrium bond length of ∼1.4 Å; (middle) at the transition state, with a bond length of ∼1.8 Å; (right) after bond cleavage, at a bond length of ∼2.2 Å.

transition state where the barrier height is a maximum. Here the electron spreads throughout the whole molecule, including the $C_{3'}$–$O_{3'}$ bond. Finally, the right panel shows the bond at a constrained length of 2.2 Å. After bond cleavage, the two remaining fragments are the dihydrogen phosphate anion and a carbon-centered neutral radical. The excess electron is no longer around the base component and is localized mainly in the ribose, particularly around $C_{3'}$ where the bond was cleaved. Hence, the mechanism is analogous to that for the gas phase proposed by Simons. Interestingly, both the gas- and condensed-phase energies continue to decrease after the rupture of the bond. This can be understood in terms of the electrostatic repulsion between the fragmentation products (i.e., the phosphate anion and the negative charge around the ribose). Eventually, in the condensed phase these charges are screened by the solvent and the curve stabilizes. In addition, as soon as there is space for a water molecule to access the $C_{3'}$ carbon atom in the ribose, the possibility of protonation is restored. If that happens, then the excess electron would return to the base, as we previously showed.[23]

In summary, we have shown that the $C_{3'}$–$O_{3'}$ bond in solvated nucleotides is likely to cleave under ambient conditions. We examined each of the four nucleotides at the same level of theory, thus yielding comparable results. We have shown that the aqueous environment must be treated explicitly and include thermal fluctuations, as only in this case do the barriers become low enough (∼5 kcal/mol, and 10 kcal/mol for dAMP) to facilitate strand breaks.

To represent a physiological environment, it is important to begin to model the irradiation process under realistic conditions. Our simulations have included the explicit effects of the water environment, but this is only a part of the story. Larger DNA fragments are necessary to study sequencing effects. Moreover, in the nucleus of the cell, DNA is wrapped around histones to form chromatin. Thus, it is important to study DNA fragments in contact with amino acids. This is currently under investigation. Another important feature is that in the duplex, the bases of the two strands are H-bonded. We have touched on this point in our previous work,[23] but further research is necessary.

■ ASSOCIATED CONTENT

Supporting Information

Computational methods, details of the calculations, and convergence tests. This material is available free of charge via the Internet at http://pubs.acs.org.

■ AUTHOR INFORMATION

Corresponding Author

j.kohanoff@qub.ac.uk

Notes

The authors declare no competing financial interest.

■ ACKNOWLEDGMENTS

The authors thank Gleb Gribakin and Mario del Pópolo for useful discussions. J.K. thanks the Wellcome Trust for a sabbatical Flexible Travel Award, which allowed him to set up this project. All of the simulations were carried out in the HECToR Supercomputing Facility through a grant allocated to the UKCP Consortium.

■ REFERENCES

(1) Baccarelli, I.; Gianturco, F. A.; Scifoni, E.; Solov'yov, A. V.; Surdutovich, E. *Eur. Phys. J. D* **2010**, *60*, 1.
(2) Baccarelli, I.; Bald, I.; Gianturco, F. A.; Illenberger, E.; Kopyra, J. *Phys. Rep.* **2011**, *508*, 1.
(3) Boudaiffa, B.; Cloutier, P.; Hunting, D.; Huels, M. A.; Sanche, L. *Science* **2000**, *287*, 1658.
(4) Pan, X.; Cloutier, P.; Hunting, D.; Sanche, L. *Phys. Rev. Lett.* **2003**, *90*, No. 208102.
(5) Winstead, C.; McKoy, V. *J. Chem. Phys.* **2006**, *125*, No. 244302.
(6) Lyngdoh, R.; Schaeffer, H. *Acc. Chem. Res.* **2009**, *42*, 563.
(7) Siefermann, K. R.; Liu, Y.; Lugovoy, E.; Link, O.; Faubel, M.; Buck, U.; Winter, B.; Abel, B. *Nat. Chem.* **2010**, *2*, 274.
(8) Wang, C.-R.; Luo, T.; Lu, Q.-B. *Phys. Chem. Chem. Phys.* **2008**, *10*, 4463.
(9) Wang, C.-R.; Nguyen, J.; Lu, Q.-B. *J. Am. Chem. Soc.* **2009**, *131*, 11320.
(10) Li, X.; Sevilla, M.; Sanche, L. *J. Am. Chem. Soc.* **2003**, *125*, 13668.
(11) Berdys, J.; Anusiewicz, I.; Skurski, P.; Simons, J. *J. Am. Chem. Soc.* **2004**, *126*, 6441.
(12) Gu, J.; Xie, Y.; Schaeffer, H. *ChemPhysChem.* **2006**, *7*, 1885.
(13) Gu, J.; Wang, J.; Leszczynski, J. *J. Am. Chem. Soc.* **2006**, *128*, 9322.
(14) Kumar, A.; Sevilla, M. *J. Phys. Chem. B* **2007**, *111*, 5464.
(15) Li, Z.; Xheng, Y.; Cloutier, P.; Sanche, L.; Wagner, J. R. *J. Am. Chem. Soc.* **2008**, *130*, 5612.
(16) Gu, J.; Xie, Y.; Schaeffer, H. *Nucleic Acids Res.* **2007**, *35*, 5165.
(17) Gu, J.; Wang, J.; Leszczynski, J. *Nucleic Acids Res.* **2010**, *38*, 5280.
(18) Gu, J.; Wang, J.; Leszczynski, J. *J. Phys. Chem. B* **2011**, *115*, 14831.
(19) Simons, J. *Acc. Chem. Res.* **2006**, *39*, 772.
(20) Schyman, P.; Laaksonen, A. *J. Am. Chem. Soc.* **2008**, *130*, 12254.
(21) Gu, J.; Wang, J.; Leszczynski, J. *ChemPhysChem* **2010**, *11*, 175.
(22) Schyman, P.; Laaksonen, A.; Hogosson, H. *Chem. Phys. Lett.* **2008**, *462*, 289.
(23) Smyth, M.; Kohanoff, J. *Phys. Rev. Lett.* **2011**, *106*, No. 238108.
(24) Youngs, T. G. A. *J. Comput. Chem.* **2009**, *31*, 639.
(25) Smith, W.; Yong, C. W.; Rodger, P. M. *Mol. Simul.* **2002**, *28*, 385.
(26) VandeVondele, J.; Krack, M.; Mohamed, F.; Parrinello, M.; Chassaing, T.; Hutter, J. *Comput. Phys. Commun.* **2005**, *167*, 103.
(27) Martyna, G. J.; Tuckerman, M. E. *J. Chem. Phys.* **1999**, *110*, 2810.
(28) Goedecker, S.; Teter, M.; Hutter, J. *Phys. Rev. B* **1996**, *54*, 1703.
(29) Perdew, J. P.; Burke, K.; Ernzerhof, M. *Phys. Rev. Lett.* **1996**, *77*, 3865.
(30) Sprik, M.; Cicotti, G. *J. Chem. Phys.* **1998**, *109*, 7737.
(31) Swarts, S. G.; Gilbert, D. C.; Sharma, K. K.; Razskazovskiy, Y.; Purkayastha, S.; Naumentko, K. A.; Bernhard, W. A. *Radiat. Res.* **2007**, *168*, 367.